Self-Consistent Mean Field Theory of the Microphase Diagram of Block Copolymer/Neutral Solvent Blends

M. D. Whitmore* and J. D. Vavasour

Department of Physics, Memorial University of Newfoundland, St. John's, Newfoundland, Canada A1B 3X7

Received October 21, 1991

ABSTRACT: We have calculated microphase diagrams of diblock copolymer/nonselective solvent blends via the numerical solution of the equations of the self-consistent, mean field theory of polymer blends. The focus was on the dependence of the equilibrium morphology on the relative degrees of polymerization of the two blocks of the copolymers, the Flory interaction parameter, and the overall polymer and solvent concentrations. We found that the resulting phase diagrams can all be mapped very nearly onto a common diagram, with microphase boundaries which depend primarily on the relative degrees of polymerization of the two blocks in the strong segregation regime and which agree qualitatively with the earlier RPA weak segregation theory for pure copolymers very near the order–disorder transition. There were, however, significant quantitative differences even in the weak segregation regime.

1. Introduction

It is now well-known that systems comprising diblock A-*b*-B copolymers can undergo an order–disorder transition, which is frequently referred to as the microphase separation transition (MST). This transition is controlled by the total degree of polymerization of the molecules, Z, the relative volume fractions of each block, f_A and $f_B = 1 - f_A$, and the strength of the net A–B interactions, generally modeled via the Flory interaction parameter χ_{AB}. For a given pair of volume fractions, the system undergoes a transition from the disordered phase, which we designate H, to a periodic microphase at a value of the product $\chi_{AB}Z$ which depends on f_A. At least four such microstructures exist, of which three are the most widely studied.[1,2] They consist of alternating layers, which we denote L, cylinders on a hexagonal lattice, C, or spheres on a body-centered cubic lattice, S. The dominant factor determining which of these is the equilibrium structure is the volume fraction, f_A (or equivalently f_B). If $f_A \lesssim 0.2$ or $f_A \gtrsim 0.8$, then spheres form, for $0.2 \lesssim f_A \lesssim 0.35$ or $0.65 \lesssim f_A \lesssim 0.8$, then cylinders form, and for $0.35 \lesssim f_A \lesssim 0.65$, layers form. In each of the first two cases, the minority component forms the discontinuous phase. As well, PS-*b*-PI exhibits a bicontinuous "double diamond" structure in the composition range 0.27–0.38, between the cylindrical and lamellar morphologies.[1,2]

This microphase behavior can be summarized by a phase diagram which shows the equilibrium microphases and the phase boundaries as functions of $\chi_{AB}Z$ and f_A. One of the earliest theoretical treatments was by Helfand and Wasserman,[3] who calculated the phase diagram for PS-*b*-PBD. They used the self-consistent mean field theory developed by Helfand and co-workers,[4-9] as well as what they called the narrow interphase approximation (NIA). In this approximation it is assumed that the width of the interphase is much less than the sizes of the domains, an assumption which should become progressively more valid with increasing $\chi_{AB}Z$, i.e., in the strong segregation limit. For their calculations they chose a constant value of χ_{AB} and varied the copolymer molecular weight and the block weight fractions. They found phase boundaries separating the different microstructures which were almost independent of χ_{AB}, i.e., equilibrium morphologies which depended almost solely on the weight fractions. In particular, spheres were stable for PS weight fractions $w_{PS} \lesssim 0.1$ and $w_{PS} \gtrsim 0.85$, cylinders for $0.1 \lesssim w_{PS} \lesssim 0.3$ or $0.65 \lesssim w_{PS} \lesssim 0.85$, and layers for $0.3 \lesssim w_{PS} \lesssim 0.65$.

Birshtein and Zhulina have recently applied scaling theory to model copolymer/solvent blends in the strong segregation regime, incorporating swelling effects of good solvents.[10] These model systems are ones in which the pure component densities of each constituent are equal, as are the two corresponding Kuhn statistical lengths. For the case of copolymer/neutral solvents, which is the case treated in this paper, they found, in this limit, that the equilibrium morphology was independent of overall concentrations and unaffected by the swelling. The L ↔ C microphase boundaries occurred at $f_A \simeq 0.28$ and 0.72 and the C ↔ S boundaries at $f_A \simeq 0.13$ and 0.87, in good agreement with the results of Helfand and Wasserman for PS-*b*-PBD.

A series of complementary calculations for model systems in the weak segregation regime, i.e., near the MST, has been carried out, beginning with the work of Leibler.[11] He used a random phase approximation (RPA)[12] and a fourth-order expansion for the free energy, identifying the equilibrium ensemble average of the density of one component, e.g. $\langle\hat{\rho}_A(\mathbf{r})\rangle$, as the appropriate order parameter. To model the ordered microphases, he approximated $\langle\hat{\rho}_A(\mathbf{r})\rangle$ by

$$\langle\hat{\rho}_A(\mathbf{r})\rangle = \sum_{\mathbf{k}_n}{}' \rho_n e^{i\mathbf{k}_n\cdot\mathbf{r}} \qquad (1)$$

with the sum restricted to wavevectors with magnitude k^*. Here k^* is the wavenumber at which the instability first occurs.

For these model systems he found that the phase diagram was completely determined by two parameters, $\chi_{AB}Z$ and f_A. For perfectly symmetric copolymers, $f_A = 0.5$, the theory predicted that the order–disorder transition was second-order and occurred at $\chi_{AB}Z = 10.5$ and that layers were the only equilibrium microstructure. However, for *any* other copolymers ($f_A \neq 0.5$), the order–disorder transition was first-order and the first equilibrium microphase consisted of spheres. As $\chi_{AB}Z$ was further increased, the equilibrium morphology changed first to

0024-9297/92/2225-2041$03.00/0

cylinders and then to lamellae. The spheres occupied only a very narrow band on the phase diagram between the H and C regions, corresponding to a composition range (in f_A) of about 1%. For large $\chi_{AB}Z$ the L region extended to highly asymmetric copolymers. These features disagreed with experiment, and they differed from the calculations using the NIA.

Fredrickson and Helfand[13] extended the Leibler theory to include fluctuation effects but assuming that eq 1 still held for the thermal average density distribution. In the limit of $Z \to \infty$, all of their results reduced to those of the RPA theory of Leibler, but differences appeared for finite degrees of polymerization. The transition became first-order for all f_A, and it was shifted to larger values of $\chi_{AB}Z$. As well, small "windows" on the phase diagram opened up, through which the system passed directly from the homogeneous to the lamellar or the cylindrical phases. As these windows opened, the S region on the phase diagram became smaller. For example, for $Z = 10^9$, the H $\leftrightarrow$ L window existed for $0.49 \lesssim f_A \lesssim 0.51$ and the H $\leftrightarrow$ C window for $0.48 \lesssim f_A \lesssim 0.49$ and $0.51 \lesssim f_A \lesssim 0.52$, but the rest remained H $\leftrightarrow$ S. For $Z = 10^6$, the windows opened slightly further, to $0.475 \lesssim f_A \lesssim 0.525$ for the H $\leftrightarrow$ L window and to $0.42 \lesssim f_A \lesssim 0.475$ and $0.525 \lesssim f_A \lesssim 0.58$ for H $\leftrightarrow$ C. For $Z = 10^4$, the H $\leftrightarrow$ L window opened to $0.43 \lesssim f_A \lesssim 0.57$, but the spherical morphology disappeared completely from the phase diagram. We interpret this work as indicating that, at least near the order–disorder transition, fluctuation effects are important but that the predicted phase diagrams still exhibit apparently anomalous features.

Mayes and Olvera de la Cruz[14,15] extended the work of Leibler and Fredrickson and Helfand by including up to three higher order harmonics in the density, i.e., in eq 1, both with[15] and without[14] fluctuation effects included. In both cases, they used fourth-order expansions of the free energy. In the first case[14] they calculated the variation in the lattice constant near the order–disorder transition, e.g., the layer thickness in the lamellar structure. In the second paper,[15] Olvera de la Cruz compared the free energies of different structures, including a three-dimensional hexagonal close packed structure (hcp). The analysis suggested that for $Z < 10^9$, even for $f_A = 0.5$, this hcp structure, rather than the lamellae, is the equilibrium morphology near the order–disorder transition.

The work summarized above used either the NIA, applicable to the strong segregation regime,[3] or fourth-order approximations to the free energy with the thermal average density variations described by a limited number of wavevectors. An alternative approach, which we use in this paper, is to numerically solve the equations of the self-consistent mean field theory,[16-20] with no a priori assumption about the shape of the equilibrium density profiles, without assuming the NIA, and without truncating the free energy expression to fourth-order. The approach has indicated, for example, that the copolymer density profiles in copolymer/neutral solvent blends are cosine-like, and the amplitudes of the density variations are small, only over limited ranges very near the MST.[16,18] As well, it predicted that the lamellar thickness in these blends scales faster with copolymer molecular weight in the weak segregation regime than in the strong segregation regime,[18] in apparent agreement with recent measurements on pure copolymers.[21] The primary approximations of the approach are its neglect of fluctuations,[13,15] equation of state effects, and swelling effects of good solvents.[10]

The goal of this paper is to provide a contribution to our understanding of these systems, by calculating the phase diagram of copolymer/neutral solvent blends via numerical self-consistent calculations for the three common structures, L, C, and S, as functions of the total degree of polymerization of the copolymers, relative degrees of polymerization of the two blocks, Flory interaction parameter χ_{AB}, and overall copolymer and solvent concentrations. For simplicity we assume that the Kuhn statistical lengths for the two blocks and the molecular volumes for both the monomers and the solvent molecules are equal, as was done in most of the earlier work. This could very easily be generalized.

2. Formalism

The goal is to identify the equilibrium structure for each copolymer/solvent blend. A given blend is specified by the total degree of polymerization, Z, the degree of polymerization of each block, Z_A and $Z_B = Z - Z_A$, the overall copolymer and solvent volume fractions $\bar{\phi}_c$ and $\bar{\phi}_s = 1 - \bar{\phi}_c$, and the interaction parameters χ_{AB}, χ_{SA}, and χ_{SB}. Since we assume that all bulk densities, ρ_{0p}, are equal, as are the two Kuhn statistical lengths, b_p, the copolymer volume fractions are simply $f_A = Z_A/Z$ and $f_B = Z_B/Z$.

We need to calculate the equilibrium free energy relative to the disordered phase of each of the three possible structures, S, C, and L. For each case, the system is assumed to form an infinite periodic microphase, described by a set of lattice vectors $\mathbf{R}_n$ and associated unit cell of volume Ω. To calculate the free energy, we solve the self-consistent problem for the density distributions and potentials $w_p(\mathbf{r})$, for p = A, B, and S. This is described fully in ref 18. In brief, we need to solve the diffusion equation for periodic polymer distribution functions denoted $\tilde{Q}_p(\mathbf{r},\tau|\mathbf{r}')$

$$\left[-\frac{b_p^2}{6}\nabla^2 + \omega_p(\mathbf{r})\right]\tilde{Q}_p(\mathbf{r},\tau|\mathbf{r}') = -\frac{\partial}{\partial\tau}\tilde{Q}_p(\mathbf{r},\tau|\mathbf{r}') \qquad (2)$$

for p = A and B, subject to initial conditions

$$\tilde{Q}_p(\mathbf{r},0|\mathbf{r}') = \sum_n \delta(\mathbf{r} - \mathbf{r}' - \mathbf{R}_n) \qquad (3)$$

From $\tilde{Q}_p$ the related functions q_p are constructed by integrating over one unit cell

$$q_p(\mathbf{r},\tau) = \int_\Omega d\mathbf{r}'\, \tilde{Q}_p(\mathbf{r},\tau|\mathbf{r}') \qquad (4)$$

These quantities also satisfy the diffusion equation but are subject to the initial condition

$$q_p(\mathbf{r},0) = 1 \qquad (5)$$

It is sufficient to solve for $\tilde{Q}_p$ and q_p in one unit cell. From these the local polymer volume fractions are calculated via convolutions

$$\phi_A(\mathbf{r}) = \frac{\bar{\phi}_A}{Z_A Q_C}\int_0^{Z_A} d\tau\, q_A(\mathbf{r},\tau)\int_\Omega d\mathbf{r}'\, \tilde{Q}_A(\mathbf{r},Z_A-\tau|\mathbf{r}')q_B(\mathbf{r}',Z_B) \qquad (6)$$

for component A and a corresponding expression for $\phi_B(\mathbf{r})$. The quantity Q_C is given by

$$Q_C = \frac{1}{\Omega}\int_\Omega d\mathbf{r}\, q_A(\mathbf{r},Z_A)q_B(\mathbf{r},Z_B) \qquad (7)$$

The local solvent volume fraction is calculated from the incompressibility condition

$$\phi_A(\mathbf{r}) + \phi_B(\mathbf{r}) + \phi_S(\mathbf{r}) = 1 \qquad (8)$$

everywhere.

The periodic potentials $\omega_p(\mathbf{r})$ are needed to solve the diffusion equations. They are given by

$$\omega_A(\mathbf{r}) = \frac{\rho_{0S}}{\rho_{0A}}\left\{\ln\left(\frac{\bar{\phi}_S}{\phi_S(\mathbf{r})}\right) + (\chi_{AB}-\chi_{SB})\left[\phi_B(\mathbf{r}) - \bar{\phi}_B + \frac{\sigma^2}{6}\nabla^2\phi_B(\mathbf{r})\right] + \chi_{SA}\left\{[\phi_S(\mathbf{r}) - \bar{\phi}_S] - [\phi_A(\mathbf{r}) - \bar{\phi}_A] + \frac{\sigma^2}{6}[\nabla^2\phi_S(\mathbf{r}) - \nabla^2\phi_A(\mathbf{r})]\right\}\right\} \quad (9)$$

for ω_A and by a similar expression for ω_B. The interactions are represented using Flory parameters $\chi_{pp'}$, defined using the solvent for the reference density, but also including gradient terms representing finite range interactions. These are modeled approximately by the finite range parameter σ, which we have taken to be equal to the Kuhn length.

For a given structure and an assumed lattice constant, i.e., domain spacing, eqs 2–9 constitute a self-consistent problem. When it is solved, the reduced free energy per unit volume, relative to a uniform melt, is calculated via

$$\frac{\Delta F}{\rho_{0S}k_BT} = \frac{1}{\Omega}\int_\Omega d\mathbf{r}\left\{\chi_{SA}\left[\phi_S(\mathbf{r})\phi_A(\mathbf{r}) - \bar{\phi}_S\bar{\phi}_A - \frac{\sigma^2}{6}\nabla\phi_S(\mathbf{r})\cdot\nabla\phi_A(\mathbf{r})\right] + \chi_{SB}\left[\phi_S(\mathbf{r})\phi_B(\mathbf{r}) - \bar{\phi}_S\bar{\phi}_B - \frac{\sigma^2}{6}\nabla\phi_S(\mathbf{r})\cdot\nabla\phi_B(\mathbf{r})\right] + \chi_{AB}\left[\phi_A(\mathbf{r})\phi_B(\mathbf{r}) - \bar{\phi}_A\bar{\phi}_B - \frac{\sigma^2}{6}\nabla\phi_A(\mathbf{r})\cdot\nabla\phi_B(\mathbf{r})\right] + \phi_S(\mathbf{r})\ln\left(\frac{\phi_S(\mathbf{r})}{\bar{\phi}_S}\right) - \frac{\rho_{0A}}{\rho_{0S}}\omega_A(\mathbf{r})\phi_A(\mathbf{r}) - \frac{\rho_{0B}}{\rho_{0S}}\omega_B(\mathbf{r})\phi_B(\mathbf{r})\right\} - \frac{\bar{\phi}_C}{r_A+r_B}\ln Q_C \quad (10)$$

Here ρ_{0p} is the density of pure component p (monomers per unit volume), k_B the Boltzmann constant, and T the temperature. Also appearing in eq 10 are r_A and r_B, defined by

$$r_p = Z_p(\rho_{0S}/\rho_{0p}) \quad (11)$$

with p = A or B. Equations 9–11 simplify in this paper because of our choices of ρ_{0p}, χ_{SA}, and χ_{SB}.

The procedure was as follows. Each blend was specified by $\bar{\phi}_c$, Z, f_A, and the interaction parameters χ_{AB}, χ_{SA}, and χ_{SB}. For each blend, and for each of the three structures L, C, and S, we performed a set of self-consistent calculations for a range of lattice parameters and found the values which minimized the free energies, say ΔF_L, ΔF_C, and ΔF_S. We then generated a set of three corresponding free energy curves, e.g., $\Delta F_L(f_A)$, by varying f_A but with the other variables held constant. For each f_A we identified the structure corresponding to the lowest free energy as the equilibrium morphology, with the phase boundaries corresponding to the values of f_A where two free energy curves crossed. We then repeated the entire process for other points on the phase diagram, i.e., for different $\bar{\phi}_c$, χ_{AB}, or Z.

In the layered structure, the problem is one-dimensional with period d; hence, we needed to solve for the functions $Q_p(x,\tau|x')$ and $q_p(x,\tau)$ in the spatial interval $[0,d]$ and for $\tau\epsilon[0,Z_p]$. For the other structures, we approximated the unit cell by a cylinder or sphere with the appropriate area or volume. In all cases we solved the diffusion equation and carried out the convolutions of eq 6 with sufficient accuracy that the average density was correct to one part in 10^9, and we iterated until the successive potentials disagreed by no more than $\pm 10^{-7}$ at any point. We estimated that the phase boundaries (within the limitations of the model) were located to within $\Delta f_A \simeq \pm 0.002$.

Table I
Systems for Which Phase Diagrams Were Calculated

Z	$\bar{\phi}_c$	χ_{AB}
1000	0.2	0.05–0.4
500	0.4	0.05–0.4
250	0.8	0.05–0.4
250	0.1–0.8	0.4
100–800	0.25	0.4

3. Results

As summarized in Table I, we have calculated five separate phase diagrams. In three of them, the total degree of polymerization of the copolymers and the overall concentrations were held constant and the value of χ_{AB} was varied. In the fourth, Z and χ_{AB} were held constant while the overall concentrations were varied, and in the final one, Z was the quantity that was varied. As indicated, this explored variations in Z of a factor of 10, copolymer concentrations ranging from about 0.1 to 0.8, and χ_{AB} as small as about 0.05.

In all cases we assumed a perfectly nonselective solvent, $\chi_{SA} = \chi_{SB}$, and in fact for these calculations we set them to zero, corresponding to an athermal solvent. On the basis of earlier work on solvent effects on the lamellar structure,[18] we expect that this last approximation would not significantly affect the structure of the phase diagrams calculated using mean field theory. This would also be consistent with the work of Birshtein and Zhulina for the strong segregation limit.[10] We note, however, that verifying this for the mean field theory remains for the future.

A basic result of the calculations is that all of these phase diagrams can be illustrated in terms of two quantities, $\bar{\phi}_c\chi_{AB}Z$ and f_A, and when expressed in this way, they all turned out to be very similar. In particular, for all $\bar{\phi}_c\chi_{AB}Z > 11$, the variation in the phase boundaries from diagram to diagram corresponding to a given value of $\bar{\phi}_c\chi_{AB}Z$ always satisfied $|\delta f_A| < 0.01$. Given the approximations inherent in mean field theory, the small differences that did appear should not be considered significant. To this extent, the dominant effect of the solvent can be thought of as simply reducing the interaction parameter to an effective value, $\chi_{eff} = \bar{\phi}_c\chi_{AB}$, which is the dilution approximation. (We emphasize, however, that we did not use this approximation in these calculations.) Consistent with this, the solvent density was relatively constant throughout the domains, as discussed in detail for the lamellar structure in ref 18. The variations in $\phi_s(\mathbf{r})$ found here were similar in magnitude to those found in that reference.

Figure 1 shows three superimposed phase diagrams corresponding to the first three cases of Table I, ranging from the vicinity of the order–disorder transition to the strong segregation regime with $\bar{\phi}_c\chi_{AB}Z = 80$. Qualitatively, they can be described as agreeing with the Leibler RPA theory in the limit of the order–disorder transition and with the NIA results of Helfand and Wasserman[3] and Birshtein and Zhulina[10] far from the MST.

For perfectly symmetric copolymers, we located the order–disorder transition for each structure by fixing f_A at 0.5 and calculating ΔF_L, ΔF_C, and ΔF_S as a function of either Z, $\bar{\phi}_c$, or χ_{AB}, as appropriate for the phase diagram being calculated. We found that in all five cases the three curves reached zero at values of $\bar{\phi}_c\chi_{AB}Z$ which agreed with each other to within ± 0.05, with the lamellar morphology consistently having a slightly lower free energy away from this point. Thus, the calculations are consistent

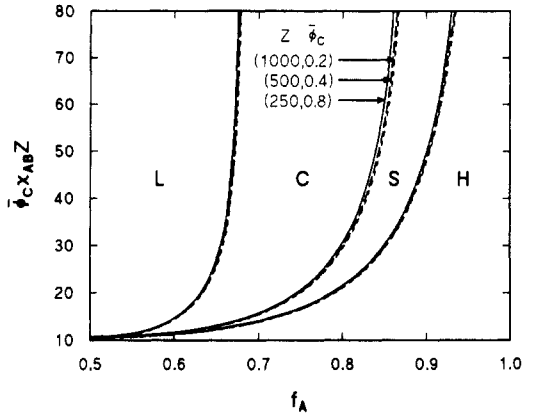

Figure 1. Calculated phase diagrams for the first three blends of Table I, as a function of volume fraction of the A block of the copolymers, $f_A = Z_A/Z$. In each of these cases, $\bar{\phi}_c$ and Z were held constant, while χ_{AB} and f_A were varied.

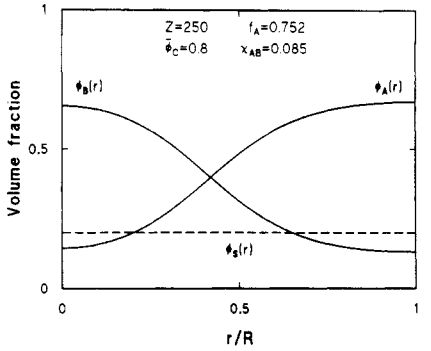

Figure 2. Calculated density profiles for the copolymer constituents, $\phi_A(\mathbf{r})$ and $\phi_B(\mathbf{r})$, and solvent, $\phi_S(\mathbf{r})$, for the blend with $\bar{\phi}_c$, Z, f_A, and χ_{AB} as shown, and block degrees of polymerization $Z_A = f_AZ$ and $Z_B = Z - Z_A$, for the spherical structure. The S ↔ H order–disorder transition occurred at $f_A = 0.753$. In this figure, R is the radius of the approximate unit cell. The interiors of the spheres are the B-rich subdomains, while the regions between these cores are A-rich. The solvent density is distributed nearly uniformly throughout the system.

with the lamellae being the only equilibrium morphology for perfectly symmetric copolymers. The actual location of this transition varied slightly from system to system. Expressing this location as $\bar{\phi}_c\chi_{AB}Z = 10.5 + \Delta$, we found values of Δ ranging from about 0.05 for the first case of Table I to 0.3 for the last case. This effect is due to the slightly nonuniform distribution of the solvent at the transition, an effect that would be missed by the dilution approximation. Consistent with ref 18, these effects, reflected in the value of Δ in this case, tended to be largest for volume fractions on the order of $\bar{\phi}_c \simeq 0.5$ and for low copolymer degrees of polymerization.

As in Leibler's results for pure copolymers, we found that for $f_A \neq 0.5$ the first ordered microphase was always S. However, even near the order–disorder transition, these phase diagrams differ significantly from those produced by previous weak segregation theories. In particular, whereas the earlier theories produced narrow C and very narrow or nonexistent S regions, in the current work, for values of $\bar{\phi}_c\chi_{AB}Z$ on the order of 14 and larger the phase boundaries turn upward smoothly but quickly, resulting in much broader C and S regions and a correspondingly narrower L region. In the strong segregation regime, the microphase boundaries become nearly vertical, i.e., only weakly dependent on $\bar{\phi}_c\chi_{AB}Z$, and are located near $f_A \simeq 0.65$ (L ↔ C transition) and $f_A \simeq 0.85$ (C ↔ S transition). These are close to the values of Birshtein and Zhulina quoted above.[10] As well, even though there is no direct window from the disordered phase to either C or L (except for $f_A = 0.5$), the intervening regions are very narrow, especially the S phase for $f_A \lesssim 0.75$.

Each self-consistent calculation produced an accompanying set of density profiles. Figure 2 shows the set for a system with $Z = 250$, $\chi_{AB} = 0.085$, $\bar{\phi}_c = 0.8$, and $f_A = 0.752$, which gives $\bar{\phi}_c\chi_{AB}Z = 17$ (and $\bar{\phi}_A \simeq 0.60$ and $\bar{\phi}_B \simeq 0.20$). In this case, the spherical morphology has the lowest free energy, with the smaller B blocks found preferentially in the cores of the spheres. The order–disorder transition occurred for this blend at $f_A = 0.753$, and so this figure corresponds to a system virtually at the S ↔ H transition, where the approximations of the weak segregation theories might be expected to be very accurate. However, we found the variations in the A and B density profiles to be quite large; $\phi_A(\mathbf{r})$ varied from 0.15 at the center of the sphere to 0.67 at the boundary of the unit cell, while $\phi_B(\mathbf{r})$ varied from 0.65 to 0.13. Given these large density variations, it is not surprising that the high-order effects included in the self-consistent theory made significant contributions to the delicate differences between the free energies of the competing structures and so modified the phase diagram even near the MST. The magnitudes of the variations in $\phi_A(\mathbf{r})$ and $\phi_B(\mathbf{r})$ for systems along the S ↔ H boundary, and so these effects, decreased or increased as f_A tended toward or away from 0.5, respectively.

To conclude, we have calculated five microphase diagrams for model diblock copolymer/neutral solvent blends via the self-consistent mean field theory of copolymer/solvent blends, sweeping through a wide range of degrees of polymerization, overall polymer concentrations, and interaction parameters. The results could be summarized in terms of two quantities, $\bar{\phi}_c\chi_{AB}Z$ and $f_A = Z_A/Z$, and when expressed in these terms, the phase diagrams were all nearly the same. Except near the MST, the equilibrium microphases depended primarily on the copolymer composition f_A only, i.e., were largely independent of $\bar{\phi}_c\chi_{AB}Z$, and the phase boundaries occurred at values of f_A which are consistent with experiments. Even near the order–disorder transition, the resulting phase diagrams differed significantly from those predicted by previous weak segregation theories, and the spatial variation of each polymer density profile was quite large. The results suggest that to understand the microphase diagram of copolymers, even in the weak segregation regime, the higher order effects included in the self-consistent theory must be included. A full theoretical understanding of this regime, including these and fluctuation effects, remains a challenge. In any event, the results presented here suggest that it might be interesting to experimentally probe this phase diagram in the weak segregation regime by varying solvent concentration.

We end with the speculation that since the phase diagrams mapped smoothly from $\bar{\phi}_c \simeq 0.1$ to $\bar{\phi}_c = 0.8$, then the calculated phase diagram for $\bar{\phi}_c = 1$, i.e., pure copolymers, would be similar. This study is currently under way and will be the subject of a later paper.

Acknowledgment. We thank Drs. K. M. Hong and J. Noolandi for early contributions to this work and Dr. M. Banaszak for contributions to the numerical work. The work was supported in part by the Natural Sciences and Engineering Research Council of Canada.

References and Notes

(1) Hasegawa, H.; Tanaka, H.; Yamasaki, K.; Hashimoto, T. *Macromolecules* **1987**, *20*, 1651.

(2) Thomas, E. L.; Alward, D. B.; Kinning, D. L.; Martin, D. L.; Handlin, D. L., Jr.; Fetters, L. J. *Macromolecules* **1986**, *19*, 2197.
(3) Helfand, E.; Wassermann, Z. R. In *Developments in Block Copolymers*; Goodman, I., Ed.; Elsevier: New York, 1982; Vol. 1.
(4) Helfand, E. In *Recent Advances in Polymer Blends, Grafts and Blocks*; Sperling, L. H., Ed.; Plenum: New York, 1974.
(5) Helfand, E. *Macromolecules* **1975**, *8*, 552.
(6) Helfand, E. *J. Chem. Phys.* **1975**, *62*, 999.
(7) Helfand, E.; Wassermann, Z. R. *Macromolecules* **1976**, *9*, 879.
(8) Helfand, E.; Wassermann, Z. R. *Macromolecules* **1978**, *11*, 960.
(9) Helfand, E.; Wassermann, Z. R. *Macromolecules* **1980**, *13*, 994.
(10) Birshtein, T. M.; Zhulina, E. B. *Polymer* **1990**, *31*, 1312.
(11) Leibler, L. *Macromolecules* **1980**, *13*, 1602.
(12) de Gennes, P.-G. *Scaling Concepts in Polymer Physics*; Cornell University Press: Ithaca, NY, 1979.
(13) Fredrickson, G. H.; Helfand, E. *J. Chem. Phys.* **1987**, *87*, 697.
(14) Mayes, A. M.; Olvera de la Cruz, M. *Macromolecules* **1991**, *24*, 3975.
(15) Olvera de la Cruz, M. *Phys. Rev. Lett.* **1991**, *67*, 85.
(16) Noolandi, J.; Hong, K. M. *Ferroelectrics* **1980**, *30*, 117.
(17) Hong, K. M.; Noolandi, J. *Macromolecules* **1981**, *14*, 727.
(18) Whitmore, M. D.; Noolandi, J. *J. Chem. Phys.* **1990**, *93*, 2946.
(19) Vilgis, T.; Noolandi, J. *Macromolecules* **1990**, *23*, 2941.
(20) Shull, K. R.; Kramer, E. J. *Macromolecules* **1990**, *23*, 4769.
(21) Almdal, K.; Rosedale, J. H.; Bates, F. S.; Wignall, G. D.; Fredrickson, G. H. *Phys. Rev. Lett.* **1990**, *65*, 1112.